International Journal of Religion
2024
Volume: 5| Number 12 | pp. 1985 – 1999
ISSN: 2633-352X (Print) | ISSN: 2633-3538 (Online)
ijor.co.uk
DOI: https://doi.org/10.61707/2w0dn528

Spatio Temporal Analysis of the Effect of Slope Gradient on the Magnitude of Erosion and Deposition in the Endikat Watershed

Dinar Dwi Anugerah Putranto[1], Agus Lestari Yuono[2], Rosidawani[3], Heni Fitriani[4], Riani Muharohmah[5]

Abstract

Erosion is a natural process caused by rainfall (R), slope gradient (λ), slope length (LS), soil type (K), and changes in land cover. These factors drive the erosion of the surface layer of the soil, intensified by steep slopes and shifts in land use. The extent of this erosion has significant implications as it contributes to a reduction in the distribution of ecosystem services (ES) both spatially and temporally in various sub-watershed areas. To analyze the magnitude of erosion, modern methodologies including the Universal Soil Loss Equation (USLE) and the refinement, the Revised Universal Soil Loss Equation (RUSLE) have been adopted particularly focusing on the slope length (LS) factor for more accurate assessments. From this analysis and the direction of deposition spatially, the results can be used to assess and consider the actual value of ES in watersheds. The results can also be used for policy in decision-making, assessing the quality and quantity of water resources, as well as managing land resources better in an economically, environmentally, and socially beneficial manner. Therefore, this study aimed to analyze the classification of the magnitude of slope in the RLKSi equation to predict the estimated spatial pattern of both erosion and deposition as well as assess the level of vulnerability to soil loss in the Endikat sub-watershed which was upstream of the Lematang watershed. The equation used was SEDRET which included the level of soil resistance to the magnitude of soil loss (RUSLE) minus actual erosion (USLE). The results of the highest erosion value of 2,205.14 tons/Ha/year occurred in an area with slope of > 45% and soil type Association & yellow brown podzolic with shrub land use. Although the highest eroded retention rate of - 6,710.17 tons/Ha/year occurred on slope of 39.09% with yellowish brown podzolic soil type and dry agricultural land use. Additionally, the area experiencing the greatest sedimentation occurred on slope of 5.79% with Andosol Brown & Regosol soil types as well as shrub land use.

Keywords: *Ecosystem Services, Erosion, Slope Length, Slope.*

INTRODUCTION

Erosion is the removal of the topsoil due to the kinetic energy generated by rainfall and flowing water (Putranto et al, 2017). When erosion occurs, the impact is not limited to the location where it happens but also affects the direction in which sediment flows and deposits. The negative impact at the erosion site is the loss of the fertile layer on the soil surface, which is carried away during the process. Furthermore, the negative impact at the location where erosion sediment flows includes the accumulation of sedimentation. When sedimentation accumulates in a river flow, it reduces the river's capacity and increases the potential for the river to overflow in the surrounding area (Davit et al, 2020). Erosion process consists of three stages namely detachment, transportation, and deposition of eroded soil particles. Five factors influence the magnitude of erosion in an area namely rainfall, soil erodibility, slope length and steepness, type of land cover, as well as land management practices (Andualem et all, 2023). The RUSLE method predicts the magnitude of erosion considering these

[1] Department of Civil Engineering and Planning, Main Area of Expertise Geomatic Engineering, Faculty of Engineering, Sriwijaya University, Jl. Raya Palembang-Prabumulih Km. 32, Inderalaya, South Sumatera, Indonesia. E-mail: dinar.dputranto@gmail.com, ORCID: https://orcid.org/0000-0001-7061-708X

[2] Department of Civil Engineering and Planning, Main Area of Expertise Water Resources Management, Faculty of Engineering, Sriwijaya University. E-mail: aguslestariyuono@ft.unsri.ac.id, ORCID: https://0rcid.org/0009-0002-7278-2083

[3] Departement of Civil Engineering and Planning, Main Area of Expertise Structural Engineering, Faculty of Engineering, Sriwijaya University, Indonesia. E-mail: rosidawani@ft.unsri.ac.id ORCID: https://orcid.org/0000-0003-4300-9227

[4] Department of Civil Engineering and Planning, Main Area of Expertise Infrastructure Management, Faculty of Engineering, Sriwijaya University. E-mail: heni.fitriani@unsri.ac.id ORCID: https://orcid.org/0000-0003-1530-1271

[5] Department of Civil Engineering and Planning, Main Area of Expertise Water Resources Management Faculty of Engineering, Sriwijaya University, E-mail: rianimuharomah@ft.unsri.ac.id ORCID: https://orcid.org/0000-0002-2815-3792

five factors, enabling the measurement of erosion in a given area. The steeper slope, the higher the quantity of inappropriate land use, and the greater the amount of rainfall, the more significant the erosions.

The USPED (Unit Stream Power Erosion and Deposition) method is a two-dimensional erosion prediction method that not only estimates the magnitude of erosion for specific areas but also predicts the direction of sediment flow and the locations of sediment deposition.

USPED assumes that sediment transport on slopes has a limited capacity and that the rate of sediment transport is determined by surface flow rather than the supply of soil particles being carried.

LITERATURE REVIEW

Various empirical soil erosion models were developed and implemented, using a Geographic Information System (GIS) based on information collected through watershed component factors (Liu and Chu, 2018). The basis for the development of soil erosion models was the USLE or soil loss equation which predicted average annual soil loss as a product of five factors namely rainfall erosivity index, soil erodibility, slope length and steepness, land cover, as well as land management factors (Olorunfemi, 2020).

In several previous reviews, Shrestha (2023) developed a hydrological distribution model using remote sensing and GIS to analyze changes in assessing runoff caused by land use changes in the Khatmandu Hill Watershed, Nepal. In the study, the spatial distribution model was developed with the SCS curve to access surface runoff variables and create alternative land use scenarios. Syam et al (2021) also developed erosion management interface used to predict the amount of erosion in watershed, providing estimates of runoff. This study provided a state-of-the-art review of current trends in the use of GIS and Remote Sensing to analyze the effects of land use changes using spatiotemporal data. The analysis also calculated and predicted erosion values for each variation of slope gradient in the study area. Furthermore, it focused on the influence of the m coefficient which affected the LS factor. The analysis also expanded the variation of the m coefficient value proposed by Weischmeier & Smith (1978) to determine whether other variations existed for slopes with gradients greater than 5%.

Erosion and deposition modeling in this study used Integrated Land and Watershed Information System (ILWIS) software. Factors that affected erosion such as rainfall, soil type, slope gradient, and land use classification were analyzed using the raster method. This study applied two erosion modeling methods namely the RUSLE method and the USPED method. In the RUSLE method, two variations were applied to compare the analysis results using the m coefficient proposed by Weischmeier & Smith (1978) with the m coefficient that included additional variations for slopes greater than 5%.

METHODOLOGY

This study aimed to provide a method capable of conducting an integrated assessment and mapping of the reduction in ecosystem services in the upstream part of the Lematang Watershed, in this case Endikat sub watershed. The novelty of this analysis lay in the holistic method to analyzing the effect of changes in slope gradient caused by land use changes from coal mining activities in the upstream and middle areas of watershed. By considering the morphometric conditions of each sub-watershed, the study estimated the amount of runoff flowing downstream. The aim was to prevent a massive increase in surface erosion and the accompanying material that would cause flooding and damage to household infrastructure and public facilities, as had happened recently (Pahlevi, 2024).

The ETM 7, TM 8+, and Sentinel 1 image interpretation methods were applied by using the D-InSAR method to obtain heights with a resolution of up to 10 m. The study obtained a more diverse analysis of erosion magnitudes in spatial and temporal modeling with more precise DTM data. Both conceptual and analytical methods were applied, compared, and discussed by using GIS methods.

Soil Conservation (SC)

The basic concept used in land deformation analysis was soil loss analysis. SC reflected the ability of different types of land use to resist erosion and maintain soil under various conditions (Li et al, 2019; Li et al, 2021). The amount of soil loss was calculated through the soil retention equation (Borselli, 2008).

$$RKLSi = Ri \cdot Ki \cdot LSi \quad (1)$$

$$USLEi = Ri \cdot Ki \cdot LSi \cdot Ci \cdot Pi \quad (2)$$

$$LS_i = \left(\frac{\lambda}{22{,}13}\right)^m (65.4\ Sin\ 2\beta + 4.56\ Sin\beta + 0.0654) \quad (3)$$

$$SEDRET_i = RKLS_i - USLE_i + Sed_{export} \quad (4)$$

Where RKLSi was the potential soil erosion (t.ha−1.yr-1), USLEi was the actual soil erosion (ton.ha−1.yr−1), Ri was erosion from rainfall (MJ•mm(ha•hr•yr)−1, Ki was the soil erosion factor (t•ha•hr.(MJ•ha)-1), LSi was slope length gradient coefficient, ƛ was area contribution to inlet of each grid cell i calculated from multiple flow direction method (m2) (Articles et al, 2021), and 22.13 was the linear dimension of grit cell in meters (according to pixel size used in DEM analysis, where 22.13 corresponded to a pixel size of 25 m), m was value for slope classification <1%, m=1; 1-3%, m=2; 3-5%, m=3; >5%, m=4; for β is slope angle in degrees (Syob, et all, 2022), Ci was infiltration coefficient of each land use, Pi was characteristic of land management aspect, SEDRETi represented soil retention against erosion, RKLSi − USLEi represented sediment resistance, and Sedexporti represented the amount of sediment intercepted upstream.

Input data for calculating SC included (Bharat et al, 2021), DEM, Land use, rainfall erosion index (R), Soil erosion index (K), land cover factor or infiltration coefficient (Ci), and land management practice factor (P). The R factor was further calculated using the monthly scale equation (Zhang, et al, 2008) which was as follows.

$$R\ = \sum_1^{12}(1,735\ x10^{\left(1,5\ \lg\frac{pi^2}{p}\right)-0,818} \quad (5)$$

Where R was erosion due to rainfall (MJ•mm(ha•hr•yr)−1, pi was monthly rainfall (mm), and P represented annual rainfall (mm). The unit of R in this formula was 100 ft•sht•in/(ac•h•y) which was then converted to the international unit MJ•mm(ha•hr•yr)−1 multiplied by 17.02. The K factor was calculated using the Soil Erodibility Equation (Zhang, et al, 2008) with the following equation.

$$K = (-0.01383 + 0.51575KEPIC) \times 0.131 \quad (6)$$

In erosion modeling using the USPED method, this study assumed that the amount of erosion depended on the sediment transport capacity of the surface flow. Although soil particles were detached due to rain when the surface flow was insufficient to transport sediment (caused by slope shape or vegetation factors), the resulting erosion was significantly reduced. The equation for sediment transport capacity was expressed as.

$$q_s\ =\ \mathrm{Kt}\ (\mathrm{A.i})^m\ \sin^n \mathrm{b} \quad (7)$$

Where q_s referred to the sediment transport capacity, Kt was the soil transportability coefficient (dependent on soil and vegetation types), m and n were constants determined by soil and flow types, A represented the contour unit width, i was the rainfall intensity, and b was slope in degrees. Erosion deposition equation was defined as the following.

$$ED = div(qs)\ = \frac{d(qs.Cos\ a)}{dx} + \frac{d(qs.Sin\ a)}{dy} \quad (8)$$

Where *a* showed the terrain surface's slope aspect (the horizontal plane's maximum slope gradient direction in degrees), and ED was erosion deposition (tons/Ha/year).

Figure 1. presented a flow diagram of the study stages in Spatio-temporal prediction of soil loss ecosystems in the Endikat sub-watershed area. The first stage was an analysis of DEM Nas data with a spatial resolution of 15 m and assisted by analysis of Sentinel 1 Satellite data with the InSAR method to obtain location heights up to a resolution of 10 m.

Study Location

The study was conducted in the Endikat sub-watershed, the upstream section of the Lematang watershed with an average elevation ranging from 300 to 800 meters above sea level. The Lematang sub-catchment formed part of the Musi River Basin in South Sumatra Province, Indonesia, situated at 2°45'–4°20' south latitude and 103°05'–104°20' east longitude.

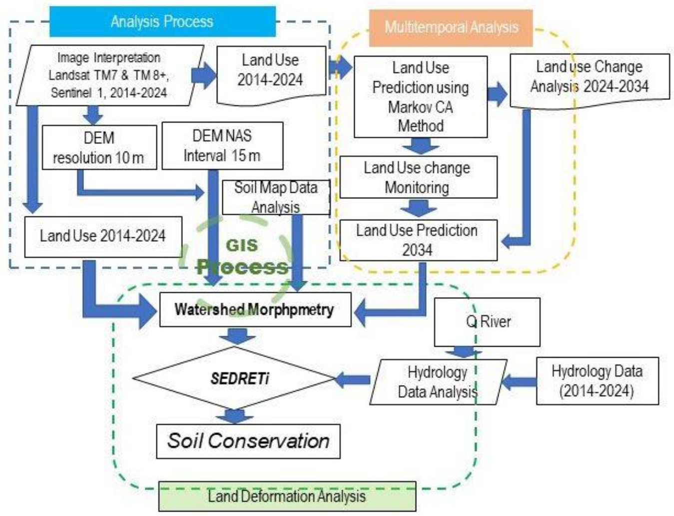

Figure 1. Research Flow Chart

The area faced high sedimentation issues in the Lematang River and tributaries due to hillside erosion and embankments created for coal mining material dumping (Putranto et al, 2016).

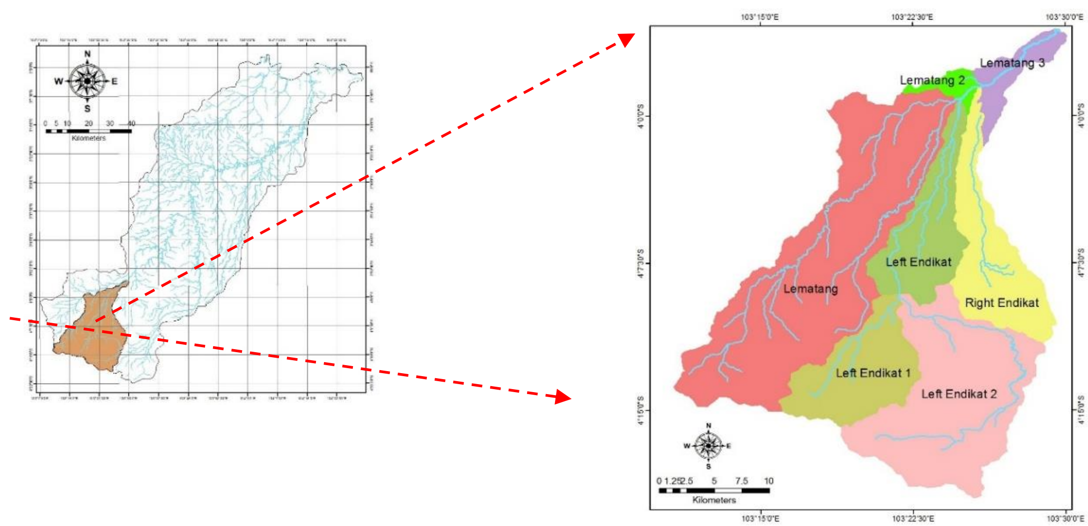

Figure 2. Study Location

The study area covered 77,912.39 hectares where the Upper Lematang Catchment exhibited slope variations between 10% and 45% and was divided into six sub-watershed. Dryland agriculture dominated the land use (38,474.82 hectares, approximately 49.40%), while the primary soil types included Brown Andosol and Regosol, covering 45,818.40 hectares (59.45% of the area). Rainfall intensity (I_{30}) for the area was 45.45 mm/hour for a 2-year return period.

RESULT AND DISCUSSION

R factor calculation

The calculation of the R factor for the return period used in erosion analysis was as follows.

I_{30} = 45,46 mm/hour (For 2 years return period)

I = 28,64 mm/hour (For 2 years intensity)

P_i = 82,60 (For a 2 year return period)

$E_i = P_i(0{,}119 + 0{,}0873\ log_{10}I)$

$= 82{,}50\ (0{,}119 + 0{,}0873\log(26{,}64))$

$= 20{,}33$

R $= E \cdot I_{30}$

$= 20{,}33 \cdot 45{,}46$

$= 924{,}41$

The calculation of the R factor for other return periods could be observed in Table 1.

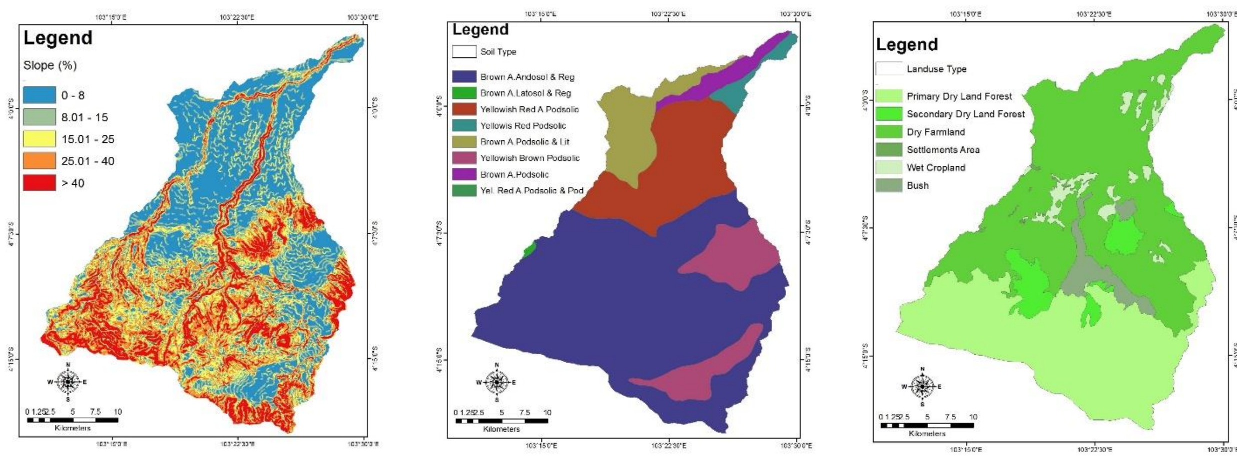

(a) (b) (c)

Figure 3. (a) Slope Classification; (b) Distribution of Soil Types; (c) Distribution of Land Use

Source : Data Analysis

Table 1. Calculation of R Factor

Return periods	*I*		Pi	Ei	R
T2	28.64	45.46	82.60	20.34	924.41
T5	37.11	58.91	107.04	27.40	1614.21
T10	42.72	67.81	123.22	32.20	2183.66
T25	49.80	79.06	143.66	38.38	3034.42
T50	55.06	87.40	158.83	43.04	3761.71
T100	60.28	95.69	173.88	47.71	4565.69

Source: Data Analysis

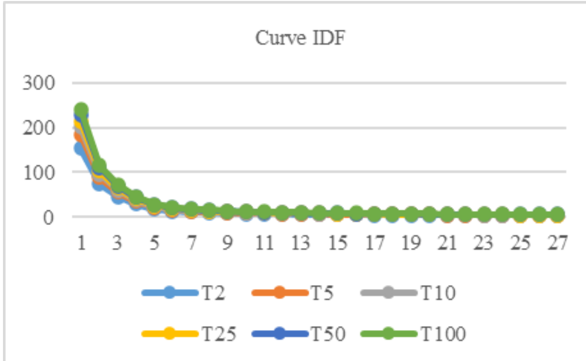

Figure 4. IDF Curve Graph of Rain Intensity I_{30} for each return period

Source: Data Analysis

RUSLE Model Erosion Analysis

In the RUSLE method modeling, spatial analysis was carried out using the following data. (a) SRTM data to derive slope information, including slope classification, slope aspect, and slope length, as well as watershed morphometry, which included flow direction, flow accumulation, delineated watersheds, and river networks. (b) Soil type classification for determining the distribution of K values. (c) TM 8+ Satellite Imagery (2024) to classify land use and determine land management factors (P). (d) BMKG daily rainfall data (2014–2024) from the North Pagar Alam Rainfall Station was used to calculate the I_{30} rainfall intensity for different return periods and determine the R-value.

Table 2. Results of Erosion Hazard Level Analysis of the Study Area

Erosion Danger Level (ton/Ha/year)	Information	Area (Ha)	Percentage (%)
0 – 15	very light	12.170,72	17,14
16 – 60	light	30.173,32	39,26
61 – 180	currently	11.673,88	15,19
181 – 480	Heavy	15.259,12	19,85
481 – 2.205,14	Very heavy	6.584,72	8,57
Total		76861,76	100

Source: Data Analysis

Table 3. Erosion Amount based on Coefficient Classification *m*

Slope (%)	*m*	Area (Ha)	Rate Erosion (ton/Ha/y)	Maximum Erosion
< 1	0,2	2.497,64	8,47	26,41
1 – 3	0,3	6.372,16	22,99	69,34
3 – 5	0,4	6.532,48	40,72	111,46
> 5	0,5	61.459,44	182,7	2.205,15
Total		76,861.72		
< 1	0,2	2.497,64	8,47	26,41
1 – 3	0,3	6.372,16	22,99	69,34
3 – 5	0,4	6.532,48	40,72	111,46

5 – 10	0,5	13.080,48	71,38	311,3
10 – 20	0,6	16.146,76	148,16	616,7
20 – 40	0,7	20.212,32	198,16	1.164,68
> 40	0,8	12.019,88	305,44	2.139,20
Total		76,861.72		

Source: Data Analysis

The results of the analysis using the RUSLE method showed that areas prone to erosion were located on the banks of the main river and other areas with steep slopes as observed in Figure 3. Based on erosion hazard classification by the Indonesian Ministry of Forestry, areas with severe and very severe hazard levels covered 15,259.12 Ha (19.85%) and 6,584.72 Ha (8.57%), respectively. The maximum erosion observed in the study area reached 2,205.14 tons/Ha/year.

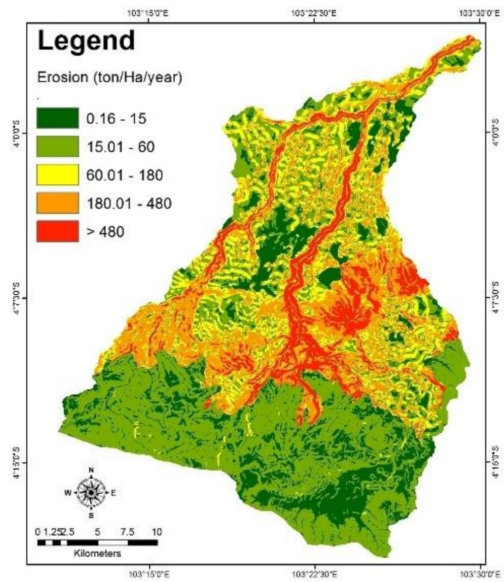

Figure 5. Distribution of Erosion at the Endikat Watershed

Source: Data Analysis

Erosion Analysis Based on Sub-Watershed

The average amount of erosion in each sub-watershed of Left Endikat was recorded at 336.75 tons/ha/year. The maximum amount of erosion was identified in the sub-watershed of Left Endikat at 2,205.14 tons/ha/year. For slopes with a value of m > 5%, the average amount of erosion was smaller than in slopes with m < 5% across all sub-watersheds. Based on land use distribution, erosion on shrubland was measured at 572.90 tons/ha/year. This occurred because shrubland was characterized by open terrain overgrown with bushes which were less capable of resisting the impact of rainfall on the land.

Table 3. Distribution of erosion in each watershed

Sub Catchment	Area	Rate Erosion	Maximum Erosion
	(Ha)	(ton/Ha/th)	(ton/Ha/th)
Lematang	29.710,53	129,77	1.392,05
Lematang 2	1.144,81	132,86	979,07
Lematang 3	2.723,69	152,79	1.000,51
Right Endikat	9.053,32	197,97	1.454,06
Left Endikat	7.772,69	336,74	2.205,15

Left Endikat 1	8.553,10	95,24	1.682,91
Left Endikat 2	18.954,25	134,84	1.552,24
Total	**77.912,39**		
Lematang	29.710,53	127,51	1.350,42
Lematang 2	1.144,81	130,91	949,79
Lematang 3	2.723,69	150,25	970,59
Right Endikat	9.053,32	194,42	1.410,58
Left Endikat	7.772,69	329,22	2.139,20
Left Endikat 1	8.553,10	93,23	1.632,59
Left Endikat 2	18.954,25	131,72	1.505,82
Total	**77.912,39**		

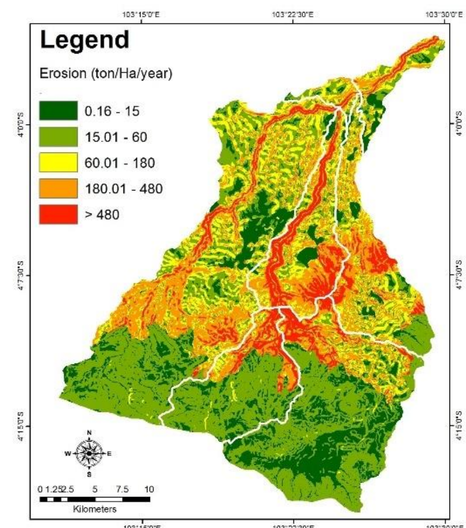

Figure 4. Distribution of erosion in each sub-watershed

Source: Data Analysis

Table 4. Results of Erosion Analysis of Each Type of Land Use

Land use	CP	Area	Erosion rate	Max. Erosion (ton/Ha/th)
Primary dryland forest	0.03	29.270,73	23,72	912,49
Secondary Dryland Forest	0.5	4.211,17	399,05	1.454,06
Settlement	0.43	202,36	77,21	1.114,99
Agriculture Dry land mixed with bushes.	0.2	38.474,82	194,42	1.894,71
Rice field	0.02	2.534,08	5,16	666,71
Shrubs	0.7	3.196,21	572,9	2.205,15
Total		77.889,38		
Primary dryland forest	0.03	29.270,73	23,17	885,2
Secondary Dryland Forest	0.5	4.211,17	389,76	1.410,57
Settlement	0.43	202,36	76,66	1.081,65

Agriculture Dry land mixed with bushes	0.2	38.474,82	190,98	1.838,05
	0.02	2.534,08	5,11	653,35
Rice field	0.7	3.196,21	559,6	2.139,20
Total		77.889,38		

Source: Data Analysis

The highest average erosion based on soil type was recorded in the brown and yellow regosol soil types at 307.22 tons/ha/year. Furthermore, the maximum erosion occurred in the red-yellow podzolic and yellow podzolic soil reaching 2,205.14 tons/ha/year.

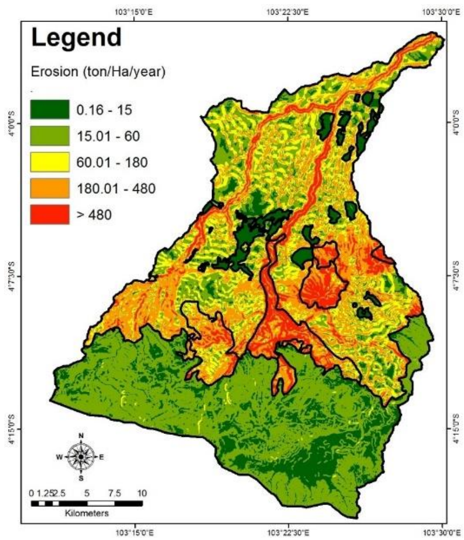

Figure 5. Erosion map of each type of Land use

Source: Data Analysis

Table 5. Results of Erosion Analysis on Soil Types

Soil Type	K	Area	Erosion rate	Maximum Erosion
Association of Brown Latosol and Brown Yellow Regosol	0.16	45.818,39	145,55	1.753,56
Association of Yellowish Red Podzolic	0.23	119,41	307,21	782,38
Association of Brown Podzolic and Litosol Yellowish Brown Podzolic	0.26	8.116,46	122,01	1.454,06
Yellowish Red Podzolic	0.26	0,34	101,38	107,65
Association of Brown Podzolic and Litosol	0.28	1.448,72	72,18	991,61
Yellowish Brown Podzolic	0.23	2.271,73	249,75	1.163,19
Association of Brown Podzolic and Podzolic	0.26	5.978,65	125,34	1.392,05
Association of Red Yellow Podzolic and Brown Yellow Podzolic	0.26	13.275,21	185,37	2.205,15
Total		77.028,91		
Brown Andosol & Regosol Association	0.16	45.818,39	142,4	1.701,12
Brown Latosol and Yellow Regosol Association	0.23	119,41	302,21	758,99
Red Yellowish Podzolic Association	0.26	8.116,46	120,04	1.410,58
Red Yellowish Podzolic	0.26	0,34	100,36	106,57
Brown Podzolic and Lithosol Association	0.28	1.448,72	71,42	961,96

Brown Yellowish Podzolic	0.23	2.271,73	244,97	1.128,41
Brown Podzolic & Podzolic Association	0.26	5.978,65	123,6	1.350,42
Red Yellowish Podzolic and Yellow Podzolic Association	0.26	13.275,21	182,01	2.139,20
Total		77.028,91		

Source: Data Analysis

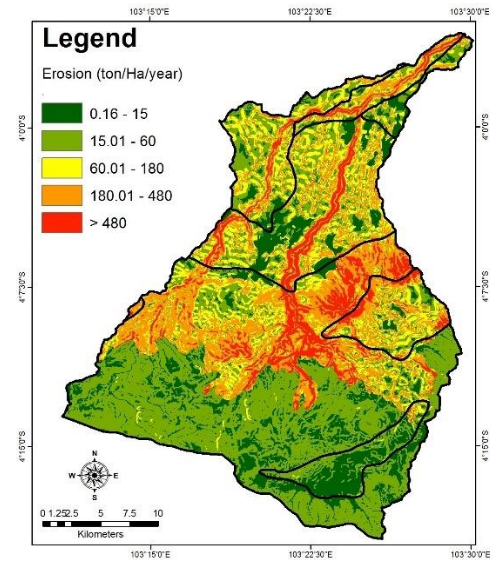

Figure 6. Erosion Map each Soil

Source: Data Analysis

USPED Method Analysis

The results of USPED modeling showed the distribution of deposition and erosion. Areas prone to erosion were found in steep slopes, river bends, and convex terrain, while sedimentation was more common in flat areas and depressions. The distribution of erosion and deposition was observed in Figure 7.

Table 6. Erosion and Deposition Analysis of the Endikat Watershed

Erosian Deposition (Ton/Ha/year)	area	Percentage
< -3.710	181,4	0.24
-3.710 - -2.227	402	0.54
-2.227 - -1.031	623,56	0.84
-1.030 - -275	1.914,84	2.57
-275 – 0	44.506,88	59.80
0 – 279	24.412	32.80
280 – 1.054	1.384,84	1.86
1.055 – 2.269	514,36	0.69
2.270 – 3.791	344,56	0.46
> 3.791	147,76	0.20
Jumlah	74.432,20	100

Source: Data Analysis

The results of deposition erosion analysis were divided into two parts, namely the eroded and deposition parts with negative and positive values respectively. The flat slope had the potential for final deposits found in an area of 15.0328 tons/Ha/year. Furthermore, the steepest slope experienced maximum erosion and was found at -36.9502 tons/Ha/year.

Table 7. Erosion and deposition based on slope

Slope Class	Slope	Area	Rate of Erosion and Deposition (ton/Ha/year)
flat	< 8	23.906,32	15,03
sloping	9 – 15	13.535,84	-8,73
currently	16 – 25	13.591,24	-18,3
Steep	26 – 40	14.211,36	-24,33
Very Steep	> 40	12.386,52	-36,95
Total		77.631,28	

Source: Data Analysis

Erosion and deposition for each Endikat Watershed

Based on the seven Catchment areas in the study, most of the locations experienced erosion with the largest in the left Endikat Watershed of -22.23 tons/Ha/year.

Table 8. Erosion and Deposition in each Endikat watershed

Watershed	Area (Ha)	Average Erosion (ton/Ha/year)
Endikat 1	29.710,53	-9,2
Endikat 2	1.144,81	-10.45
Endikat 3	2.723,69	-15,21
Right Endikat	9.053,32	-13,48
Left Endikat	7.772,69	-22,23
Left Endikat 1	8.553,10	-5,4
Left Endikat 2	18.954,25	-8,89
Total	77.912,39	

Source: Data Analysis

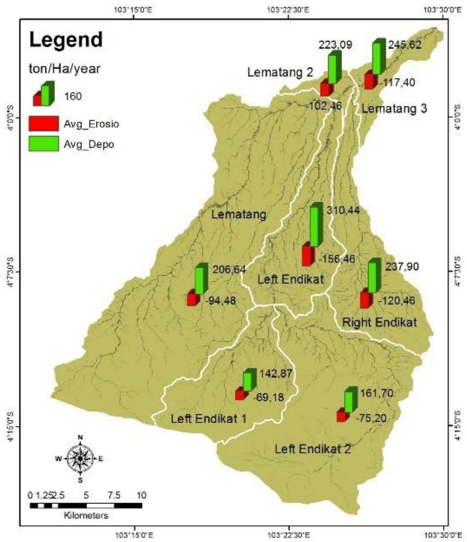

Figure 8. Erosion and deposition map of each Endikat watershed

Source: Data Analysis

Deposition Erosion Analysis Based on Land Use Type

The analysis of deposition erosion based on land use type showed that nearly all average deposition erosion values were negative, except in rice field areas.

Table 9. Deposition Erosion each Land Use Type

Land Use	Area (Ha)	Erosion/deposition rate (ton/Ha/year)
Primary dryland forest	29.270,73	-1,58
Secondary dryland forest	4.211,17	-21,56
Settlement	202,36	-8,13
Dry Land Plantation mixed with shrubs	38.474,82	-14,56
Rice field	2.534,08	1,98
shrubs	3.196,21	-31,32
Total	77.889,38	

Source: Data Analysis

These areas characterized by water flow and concave topography were more inclined to experience sedimentation than erosion. In the rice fields, the average deposition erosion value was 1.98 tons/Ha/year. The type of land use most prone to erosion was secondary dryland forest as it had only recently regenerated from bare land, leaving it with limited vegetation cover to mitigate erosion. The average deposition erosion in secondary dryland forest was recorded at -21.56 tons/Ha/year.

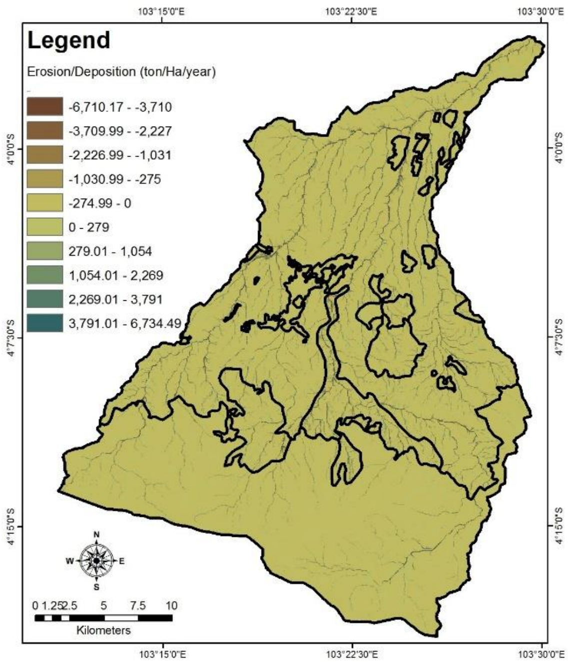

Figure 9. Erosion and deposition map each Land use type

Source: Data Analysis

Deposition Erosion Analysis Based on Soil Type

In the table of results of deposition erosion analysis based on the distribution of soil types in the study area, the study observed that all soil types exhibited a negative average deposition erosion rate. This showed that each type of soil experienced greater sediment erosion than deposition. The sub-watersheds with the highest erosion were associated with the soil type "Association of Red Yellow Podzolic and Brown Yellow Podzolic," which recorded a value of -22.23 tons/Ha/year. This result correlated with the results of the RUSLE method analysis, where the average erosion rate was also highest in the same soil type.

Table 10. Deposition Erosion Based on Soil Type

Soil Type	Area (Ha)	Average Erosion/Deposition (Ton/Ha/Year)
Association of Brown Andosols and Regosols	45.818,39	-7,91
Association of Brown Latosol and Brown Yellow Regosol	119,41	-16,03
Association of Yellowish Red Podzolic	8116,46	-2,99
Yellowish Red Podzolic	0,34	-11,76
Association of Brown Podzolic & Lithosol	1.448,72	-8,4
Yellowish Brown Podzolic	2.271,73	-25,69
Association of Brown Podzolic & Podzolic	5.978,65	-10,82
Association of Red Yellow Podzolic and Brown Yellow Podzolic	13.275,21	-17,06
Total	77.028,91	

Source: Data Analysis

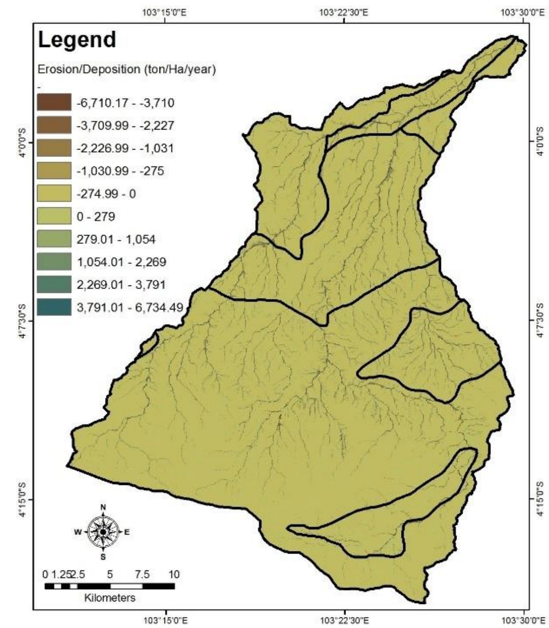

Figure 10. Erosion and deposition maps each soil type

Source: Data Analysis

CONCLUSION

In conclusion, the following points were drawn based on the results of the analysis and further discussion.

1. The results of the RUSLE and USPED method analyses showed that slope class most prone to erosion was the very steep slope (> 40%), while the least erosion occurred in the flat slope class (< 8%).
2. The highest erosion identified by the RUSLE method was 2,205.14 tons/Ha/year, occurring in an area with slope of 94.40%. This area was characterized by Red Yellow Podsolic and Brown Yellow Podsolic soils with shrubs as the dominant land use.
3. For slopes > 5%, the study recommended the reclassification of these areas as the variation in erosion magnitude remained widely distributed with significant differences in values.
4. The USPED method analysis showed that the area with the highest erosion rate of -6,710.17 tons/Ha/year was found on slopes > 40%, characterized by yellowish brown podsolic soil and dryland agriculture usage. However, the largest sediment deposits were observed on land with slope of < 6%.

ACKNOWLEDGMENTS

The authors are grateful to the Directorate of Research Technology and Community Service, Directorate General of Higher Education, Research and Technology, Ministry of Education, Culture, Research and Technology, the Republic of Indonesia, who has provided research funding through Fundamental Research grants based on Master Contract No.:090/E5/PG.02.00.PL/2024, Date : June 11, 2024.

REFERENCES

Articles. O, E. the L. F. for R. through I. S. L. P. of D. E. D. within A. Grid, R. D. Van Remortel, and R. S. & Supp, "Estimating the LS Factor for RUSLE through Iterative Slope Length Processing of Digital Elevation Data within Arclnfo GridNo Title," Cartography, vol. 30, no. 1, pp. 27–35, 2001, doi: https://doi.org/10.1080/00690805.2001.9714133.

Borselli. L, P. Cassi, and D. Torri, "Prolegomena to sediment and flow connectivity in the landscape: A GIS and field numerical assessment," CATENA, vol. 75, no. 3, pp. 268–277, 2008, doi: https://doi.org/10.1016/j.catena.2008.07.006.

Bharath.A, K. K. Kumar, R. Maddamsetty, M. Manjunatha, R. B. Tangadagi, and S. Preethi, "Drainage morphometry based sub-watershed prioritization of Kalinadi basin using geospatial technology," Environ. Challenges, vol. 5, no. August, p. 100277, 2021, doi: 10.1016/j.envc.2021.100277.

David B Camp, Peter M. Sadler and Veerle Vanacer., The human impact on North American erosion, sediment transfer, and storage in a geologic context, Nature Communication 11, Article number: 6012.

Gara Megha Shyam a, Ajay Kumar Taloor b, Sudhanshu a, Suraj Kumar Singh c, Shruti Kanga. Sustainable water management using rainfall-runoff modeling: A geospatial approach, Groundwater for Sustainable Development, Volume 15, November 2021

Jordán. A et al., "Wettability of ash conditions splash erosion and runoff rates in the post-fire," Sci. Total Environ., vol. 572, 2016, doi:10.1016/j.scitotenv.2015.09.140.

Li. Z, X. Deng, G. Jin, A. Mohmmed, and A. O. Arowolo, "Tradeoffs between agricultural production and ecosystem services: A case study in Zhangye, Northwest China," Sci. Total Environ., vol. 707, p. 136032, 2020, doi: https://doi.org/10.1016/j.scitotenv.2019.136032.

Li. Q et al., "The link between landscape characteristics and soil losses rates over a range of spatiotemporal scales: Hubei province, china," Int. J. Environ. Res. Public Health, vol. 18, no. 21, pp. 1–16, 2021, doi: 10.3390/ijerph182111044.

Liu. J, W. Liu, and K. Zhu, "Throughfall kinetic energy and its spatial characteristics under rubber-based agroforestry systems," Catena, vol. 161, 2018, doi: 10.1016/j.catena.2017.10.014.

Olorunfemi. I.E, A. A. Komolafe, J. T. Fasinmirin, A. A. Olufayo, and S. O. Akande, "A GIS-based assessment of the potential soil erosion and flood hazard zones in Ekiti State, Southwestern Nigeria using integrated RUSLE and HAND models," CATENA, vol. 194, p. 104725, 2020, doi: https://doi.org/10.1016/j.catena.2020.104725.

Pahlevi. R, "Sungai Lematang Meluap Ratusan Rumah di Pali Terendam Banjir," Detik Sumbagsel, 2024.

Shrestha, M. N. Spatially Distributed Hydrological Modelling Considering Land-Use Changes Using Remote Sensing and GIS. In Proceedings of Map Asia Conference.2023

Tesfa Gebrie Andualem, Guna A. Hewa, Baden R. Myers, Stefan Peters, and John Boland, (2023). Erosion and Sediment Transport Modeling: A Systematic Review. Land, 12, 1396. https://doi.org/10.3390/land12071396

Švob.M, D. Domínguez-Villar, and K. Krklec, "Characterization of soil drainage dynamics on karst terrains by developing a site-specific reservoir cascade scheme hydrological model with preferential flows," J. Hydrol., vol. 612, no. March, 2022, doi: 10.1016/j.jhydrol.2022.128147.

Wischmeier.D, W.H.; Smith, Predicting Rainfall Erosion Losses: A Guide to Conservation Planning. USA: Department of Agriculture, Science and Education Administration: Washington, DC, USA, 1978.

Zhang.K.L, A. P. Shu, X. L. Xu, Q. K. Yang, and B. Yu, "Soil erodibility and its estimation for agricultural soils in China," J. Arid Environ., vol. 72, no. 6, pp. 1002–1011, 2008, doi: https://doi.org/10.1016/j.jaridenv.2007.11.018.